Iraqi Journal of Veterinary Sciences

www.vetmedmosul.com

The impact of silver/beta-tricalcium phosphate nanocomposite combined with injectable platelet-rich fibrin on the healing of mandibular bone defects: An experimental study in dogs

A.I. Naser[1], R.S. Hamed[1] and G.A. Taqa[2]

[1]Department of Oral and Maxillofacial Surgery, [2]Department of Dental Basic Sciences, College of Dentistry, University of Mosul, Mosul, Iraq

Article information

Article history:
Received 05 January, 2024
Accepted 21 February, 2024
Published online 26 March, 2024

Keywords:
Nanosilver
Nanocomposite
Bone healing
i-PRF
Dogs

Correspondence:
R.S. Hamed
rshh70@uomosul.edu.iq

Abstract

This study examined the biological response of canine mandibular bone to synthetic nanocomposite material alone or combined with injectable platelet-rich fibrin i-PRF. Twelve healthy adult male local breed dogs aged 12 to 18 months and weighing 15-20 kg were used in this study. These dogs were divided into two main groups based on healing intervals of 1 and 2 months. Each interval group had four subgroups, including three dogs in each one. The division was based on the grafting material used: empty defect (Control -ve), i-PRF alone, nanocomposite alone, and i-PRF + nanocomposite. All surgeries were performed under general anesthesia. The surgical procedure began with a 5 cm parallel incision along the mandible's lower posterior border. After exposing the periosteum, three 5mm-diameter, 5-mm-deep critical-size holes were made, 5mm between each. Each group with the allocated protocol had three independent holes. The defects of all study groups were covered with resorbable collagen membranes, and then the subcutaneous tissue and skin closed routinely. Total densitometric analysis showed highly significant differences between groups, with the Nano+ i-PRF group having the highest means, 332.66 and 522.66 at 1 and 2 months. Nanocomposite and i-PRF increased and maintained bone density during the study.

DOI: 10.33899/ijvs.2024.145856.3400,

Introduction

Bone constantly remodels and repairs itself. Resident cells (osteoclasts and osteoblasts) and signalling molecules remove damaged tissue and create new bone (1-3). The bone healing process has three overlapping stages: inflammation, reparative, and remodelling (4,5). Inflammation begins when the bone breaks and lasts several days. Under the influence of cytokines, macrophages and other immune cells enter bone defects, clear bone tissue debris, and form vascular and granulation tissue (6). Bone remodelling, the penultimate phase of bone healing, takes months. This stage requires osteoblast-osteoclast interaction. Bone regains shape and restores the damaged part's geometry and function (7). The most significant advancements in bone regenerative medicine are the prerequisites for bone regeneration, the clinical usage of synthetic bone replacements, and the reduction of microbial infections (8). A synthetic biomaterial doped with metal ions that have antibacterial characteristics successfully prevents post-operative infections (9). Nowadays, dentistry employs silver nanoparticles (AgNPs) to reduce the danger of contamination and disease associated with bone augmentation. Consequently, specific forms of bone cement, scaffolds, and membranes have been infused with AgNPs (10). Bone grafts have been made from metals, polymers, ceramics, and platelet concentrates. Cells or bioactive molecules in these materials create a dynamic wound-healing environment (11). β-tricalcium phosphate is a popular and effective artificial bone graft. Osteoconductive and osteoinductive, these traits allow bone defect repair and cell-mediated resorption (12,13). Currently, platelet concentrates are employed in dental procedures to aid in healing soft and hard tissues (14). Injectable platelet-rich fibrin is a new platelet concentrate with antibacterial properties. i-PRF increases fibroblast migration, PDGF, TGF, collagen one expression, and growth factor release (15). Intra-oral radiography techniques enable easy tracking of the amount of bone repair. They are straightforward, inexpensive, non-invasive diagnostic tools used to examine internal bone changes in alveolar bone and contrast various bone densities (16). By providing better visibility and standardization than conventional radiography, digital radiography makes it easier to detect small changes in the bone (17). Hounsfield units (HU) are the standard quantities from CT imaging and usually denote the relative density of bony tissues. There are Controversies surrounding the precision of CBCT-based HU measurement. According to the research of Campos *et al*. (18), CBCT is not the best method for estimating bone mineral density. However, other authors indicated that CBCT grey values could be utilized well to measure bone density (19,20). CBCT is a reliable method for obtaining 3D pictures of oral structures. It is utilized as an alternate strategy because less radiation is produced, and it is more cost-effective (21).

In this investigation, we anticipated that using artificial nanocomposite materials alone or combined with i-PRF would aid bone healing. The current investigation aimed to determine how synthetic nanocomposite material, alone or in combination with i-PRF, affected the biological response of the canine mandibular bone.

Materials and methods

Animals

This investigation spanned two months at the Oral and Maxillofacial Surgery Department, College of Dentistry, University of Mosul. A total of 12 healthy, adult male dogs of local breed dogs were enrolled. They were bought from the local market at ages 12-18 months, weighing 15-20 kilograms. A veterinarian consultant performed routine health checks on all the animals housed in cages with adequate ventilation and access to food, water, and natural light.

Ethical consideration

The study agreed with the ethical guidelines that the Helsinki Declaration served as the foundation. A local ethical committee approved the project after evaluating ethical standards at all stages of executing operations and handling. The ethical committee accepted the study after measuring ethical criteria at all stages of performing operations and handling animals. Approval letter No. (U.O.M. Dent/A.69.22).

Materials

T-lab (PRX tube) in Turkey supplied the i-PRF tubes (10 ml) used for blood collection with Centrifuge (Hettich, Germany; Model EBA (22). Straight surgical handpiece that is transportable (Being, China). The silver/beta-tricalcium phosphate nanocomposite bone substitute powder was bought from Yanhuang Industrial Park (Guanxian, Liaocheng, Shandong, China). The collagen membrane was purchased from Bioplast-Dent Membrane (VALDMIVA/Russia).

Experimental grouping

The study was a single-blinded randomized trial in which the animals were split into two groups depending on the intervals between euthanasia: one month and two months. According to the material to be implanted into the designated bone defect in the lower border of the jaw, each interval group was divided into four subgroups (each with three dogs for each protocol to be used depicted. Empty defect (Cont. -ve) / three dogs in which three defects on one side of the mandible representing a one-month interval were created and three defects on the other side of the mandible representing a two-month interval. I-PRF alone (+ve Cont.) / three dogs in which three defects on one side of the mandible representing a one-month interval were created and three defects on the other side of the mandible representing a two-month interval. Silver/beta-tricalcium phosphate nanocomposite alone / three dogs in which three defects in one side of the mandible representing a one-month interval were created and three defects on the other side of the mandible representing a two-month interval. I-PRF plus + a silver/beta-tricalcium phosphate nanocomposite/ three dogs in which three defects on one side of the mandible representing a one-month interval were created and three defects on the other side of the mandible representing a two-month interval. I-PRF was made by centrifuging two plastic vacuum (PRX) tubes filled with a total of 2 * 10 ml of blood for 3 minutes at 700 rpm after being drawn from the jugular vein (23) of each dog with a disposable needle measuring 10 ml, 22 g, and 32 mm in size (22). i-PRF was obtained as the upper layer following the centrifugation cycle. The resulting i-PRF and nanocomposite material were mixed in a tiny glass container.

Anesthesia and surgical procedure

For anesthesia, administering atropine (0.04 mg/kg) intramuscularly (Anova/Vietnam) was crucial to reducing bronchial secretions and supporting heart rate. Immediately following this, a combination of Ketamine 10% (Gracure Pharmaceuticals Ltd, Bhiwadi, India) and Xylazine 2% (Interchemi Co, Holland) in a dose of 10mg/kg; 3mg/kg respectively injected intramuscularly. Additional doses of Ketamine are only administered if needed to maintain sufficient anesthesia (24). Once the dog was adequately anesthetized, the surgery began by making a parallel incision of 5 cm on the lower posterior border of the mandible. The periosteum was reflected to expose the inferior border of the mandible. Three circular critical-size holes, 5mm between each, for each one 5mm in diameter and 5mm in depth, were created using a 5mm diameter trephine surgical bur, as shown in (Figure 1). A plastic scoop was used for standardizing the amount of nanocomposite powder. i-PRF was mixed with nanocomposite in a glass container until it reached a gel-like consistency for easy handling. The defects were then filled with the nanocomposite material, the i-PRF, and a combination of both as the third and fourth groups were left empty as a con-ve. To ensure proper healing, the defects of all study groups were covered with resorbable collagen membranes. Finally, the subcutaneous and skin were closed using absorbable Vicryl sutures (2/0) to restore it to its original position. Ceftiofur (5 mg/kg) and diclofenac (3 mg/kg) were administered intramuscularly to the animals as a single dose to prevent infection and speed recovery, respectively. Additionally, tetracycline ointment was applied to all skin wounds.

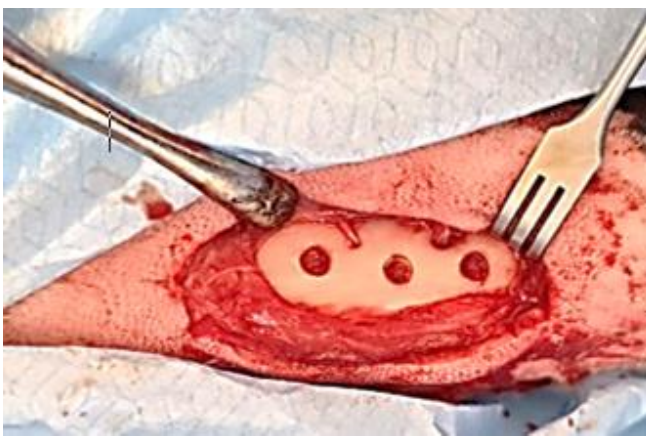

Figure 1: Surgical procedure.

Animal sacrifice

Twelve dogs were sacrificed after two months. Dogs were euthanized with an intravenous injection of pentobarbitone (1 ml/10 lbs. of body weight). The right mandible for two-month intervals and the left for one-month intervals were dissected free and fixed in 10% buffered formic acid for radiographic analysis.

Radiographic analysis

For each animal, CBCT (Large V/China) scans were performed at both intervals using the CBCT imaging machine, and the bone density was estimated in Hounsfield Units (HU) using CBCT computer system software. The following parameters were pre-adjusted before exposure: kilovoltage (Kv): 100Kv, milliamp: 6.0 mA, and exposure time: 20 sec. Two radiologists performed the radiological study after manually selecting the fault location in an axial section using the editing tool, measure, and a three-dimensional (3D) visual inspection. For each dog, the Mean data was recorded from a CBCT scan and saved in digital file format for visualization and analysis.

Statistical analysis

The Statistical Package for Social Sciences application was used for the statistical analysis (SPSS version 22.0, Chicago, IL, USA). Independent t-tests were used to compare two independent intervals, while one-way ANOVA was used to compare various groups within an interval at P<0.05.

Results

Clinical observations

Within 15 days after surgery, every skin stitch had healed. There were no adverse inflammatory or foreign-body reactions or local or systemic post-operative problems in any dog.

Radiographical

A total of 12 dogs had surgery by one surgeon. Nine dogs were implanted with different study materials, and three dogs were left without treatment. So, 36 defects were created in the lower posterior border of the mandible. In the present study, the one-month intervals showed no significant difference between Con-ve, i-PRF, and Nano groups. While, in comparison with the Nano+i-PRF group, there was a significantly different. Moreover, at two-month intervals, there was a significant difference between Con-ve and i-PRF groups with Nano and Nano+i-PRF groups. The result between intervals revealed that the Con-ve were found to be 129.33±11.67 and 140±26.21 in one and two months, respectively, as there was no significant between them. In i-PFR, there was a significance differences between the two groups to be 138±15.52 and 267±1.0 in one and two months, respectively. This is also true for the nanocomposite group, in which there was a high significance between the two groups to found to be 165.66± 31.21, 460.66±26.40 in one and two months, respectively. Regarding the i-PRF+ Nano composite group similarly, were found to be 323.66±65.95 and 522.66±67.88 in one and two months, respectively (Figures 2-4) (Tables 1 and 2).

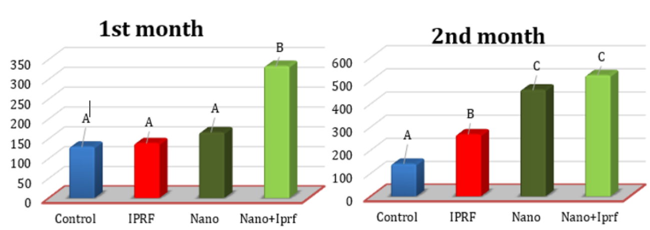

Figure 2: One-Way ANOVA for comparison of study material within groups, A (one month) and B: (two- months).

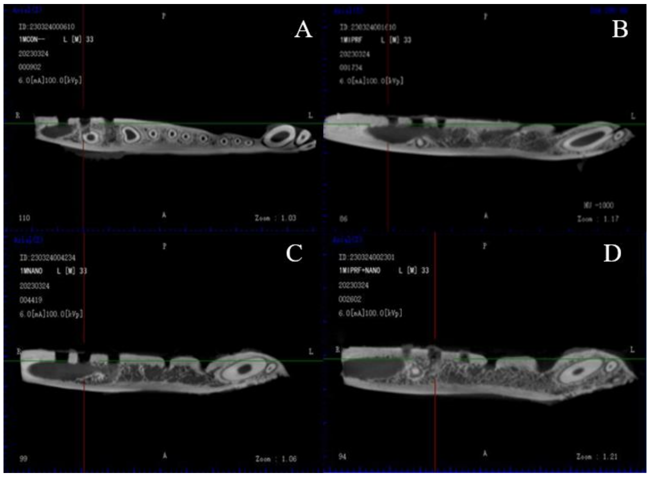

Figure 3: Cone beam compared tomography axial plane after surgical treatment with study groups at one month. A:Con-ve, B:IPRF, C:Nanocomposite, D:Nano+IPRF.

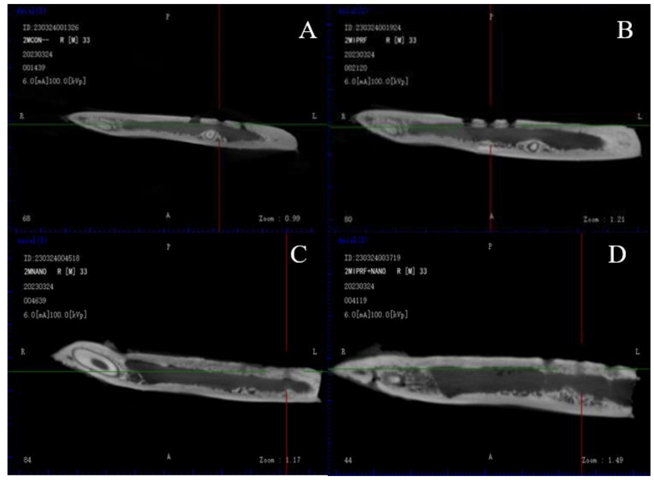

Figure 4: Cone beam compared tomography axial plane after surgical treatment with study groups at two months. A:Con-ve, B:IPRF, C:Nanocomposite, D:Nano+IPRF.

Table 1: Independent t-test for comparison of study groups during healing periods

Times	Control	i-PRF	Nano	Nano+i-PRF
One month	129.33±11.67	138±15.52	165.66± 31.21	323.66±65.95
Two months	140±26.21	267±1.0*	460.66±26.40*	522.66±67.88*
P-Value	0.55	0.000	0.000	0.025

Table 2: One-way ANOVA for comparison of study groups within interval

Groups	One - month	Two - months
Con –ve	129.33 ±11.67 A	140 ± 26.21A
i-PRF	138 ± 15.52A	267 ± 1.0 B
Nano	165.66 ± 31.21 A	460.66 ± 26.40 C
Nano+i-PRF	332.66 ± 65.95 B	522.66 ± 67.88 C
P- Value	0.001	0.000

Discussion

This study aimed to assess the bone densities of synthetic nanocomposite bone substitutes either alone or integrated with injectable platelet-rich fibrin using the radiographic outcome of CBCT. The current study proposes Several animal models for bone graft research. The benefit of using adult local breed dogs as experimental animals rather than rabbits or rats is that they provide adequately sized bone defects to hold enough graft material for various assessment motilities. Dogs also have a physiologic and metabolic activity index like primates (22). In the present study, bone density was assessed by CBCT; this result is in line with the study of Emamverdizadeh *et al.* (25); grey values could be utilized well to measure bone density (26). This was the first study comparing nanocomposite synthetic bone substitutes with i-PRF utilizing CBCT to enhance bone density. In the current study, the results of CBCT radiography for the study groups at one-month intervals showed the presence of a radiolucent zone of defects equal to some extent for Con-ve, i-PRF, and Nanocomposite groups, suggesting that low rate of bone formation in comparison with Nanocomposite with i-PRF group, the radiolucency was decreased shifting to the higher rate of bone formation. The body defends against i-PRF and Nanocomposite materials and induces inflammatory reactions as a normal healing process. However, this reaction subsided and no longer continues because the i-PRF has an antibacterial effect due to the high number of leukocytes. These results were in line with the study of Kour *et al.* in which the i-PRF has no artificial additives and has an antibacterial effect due to the high number of leukocytes in much greater concentrations along with the platelets in this kind of platelet concentrates. Also, neutrophils secrete the myeloperoxidase present in their granules. Furthermore, monocytes produce cytokines and chemotactic factors that participate in inflammation (27,28).

These effects can be explained by the low-speed concept by Ghanaati *et al.* for blood centrifugation, whereby lower centrifugation speeds contained higher numbers of cells, including leukocytes, before forming a fibrin clot (29,30). The effect of i-PRF was synergistic with silver nanoparticles (AgNPs), a part of nanocomposite material composition that reduces post-operative bacterial contamination, promoting a higher bone deposition rate and increasing the defects' radiopacities. Based on these assumptions, many studies assessed the bactericidal effect of silver nanoparticles. They concluded that the strong positive effect of AgNPs incorporating biomaterials like beta-tricalcium phosphate reduces post-operative bacterial contamination (31,32). AgNPs can pass through the outer membrane, accumulate in the inner membrane, and interact with sulfur or phosphorus groups, where their adhesion causes the cell's destabilization and damage. This increases the membrane's permeability, which causes the cell to die.

The results of this study were gone along with the study of Bee *et al.* (33) in which they concluded that the addition of silver nanoparticles to hydroxyapatite exhibits optimal antibacterial and improves the bioactive properties and promises to be used as an implant material for dental and orthopedic applications (33). The results of this study agreed with those of Zhang *et al.* (34) who evaluated the effect of I-PRF on mandibular defects in rabbits. They confirmed that the I-PRF could speed up the formation of new bone, as seen in the second month, especially in the Nanocomposite with i-PRF and Nanocomposite, by releasing more growth factors like VEGF, PDGF and RUNX 2 and enhancing angiogenesis differentiation of stem cells towards osteoblast has a significant impact on the improvement of bone regeneration (34). Because the prolonged release of nano-beta tricalcium phosphate has an antibacterial property concurrently with i-PRF, it improves bone formation owing to its impact on osteoblastic behavior, which helps when combined with a variety of biomaterials to release growth factors (35-37) significantly. These results are in line with those of Zhang *et al.* (38), who found that when beta-tricalcium phosphate biomaterials are stimulated, macrophages express fewer inflammatory factors IL-1, produce more anti-inflammatory cytokines IL-10, IL-1r, and produce growth factors VEGF, PDGF, EGF, BMP-2, and TGF-1 that collectively result in a pro-osteogenic microenvironment (39,40).

This research has clinical implications by enhancing the osteoconductive quality of synthetic bone replacements via the prolonged release of beta-tricalcium phosphate and nano silver. These characteristics will increase the success rate of dental implants by enhancing their primary stability when combined with bone transplants. The relatively brief durations of the healing periods were a shortcoming of this research, implying the existence of a longer duration. Controlling CBCT image collection was further complicated by the irregular form of the bone specimens.

Conclusion

Based on the data collected and analyzed during this investigation, it can be concluded that both nanocomposite and i-PRF successfully increased and maintained bone density during the study period, as seen by densitometric results. The current i-PRF appears to be a safe, effective, and widely accepted minimally invasive technique.

Conflict of interest

No conflict of interest, Self-funded.

Acknowledgment

We thank the College of Dentistry at the University of Mosul for supporting this research. Many thanks are also extended to the College of Veterinary University of Mosul for their assistance in this study.

References

1. Ralston SH. Bone structure and metabolism. Med. 2021;49(9):567–571. DOI: 10.1016/j.mpmed.2021.06.009
2. Wang X, Friis T, Glatt V, Crawford R, Xiao Y. Structural properties of fracture haematoma: Current status and future clinical implications. J Tissue Eng Regen Med. 2017;11(10):2864–2875. DOI: 10.1002/term.2190
3. Okamoto K, Nakashima T, Shinohara M, Negishi-Koga T, Komatsu N, Terashima A, Sawa S, Nitta T, Takayanagi H. Osteoimmunology: The conceptual framework unifying the immune and skeletal systems. Physiol Rev. 2017;97(4):1295-349. DOI: 10.1152/physrev.00036.2016
4. Abe K, Shimozaki S, Domoto T, Yamamoto N, Tsuchiya H, Minamoto T. Glycogen synthase kinase 3b biology in bone and soft tissue sarcomas. J Cancer Metastasis Treat. 2020;6(51). DOI: 10.20517/2394-4722.2020.117
5. Zhu G, Zhang T, Chen M, Yao K, Huang X, Zhang B, Li Y, Liu J, Wang Y, Zhao Z. Bone physiological microenvironment and healing mechanism: Basis for future bone-tissue engineering scaffolds. Bioact Mater. 2021;6(11):4110-40. DOI: 10.1016/j.%0Abioactmat.2021.03.043
6. Maruyama M, Rhee C, Yao Z, Goodman SB. Modulation of the inflammatory response and bone healing. Front Endocrinol. 2020;11(386). DOI: 10.3389/fendo.2020.00386
7. Wang D, Gilbert JR, Zhang X, Zhao B, Ker DF, Cooper GM. Calvarial versus long bone: Implications for tailoring skeletal tissue engineering. Tissue Eng B Rev. 2020;26(1). DOI: 10.1089/ten.TEB.2018.0353
8. Kupikowska-Stobba B, Kasprzak M. Fabrication of nanoparticles for bone regeneration: new insight into applications of nanoemulsion technology. J Mater Chem B. 2021;9(26):5221-44. DOI: 10.1039/D1TB00559F
9. Fuh LJ, Huang YJ, Chen WC, Lin DJ. Preparation of micro-porous bioceramic containing silicon-substituted hydroxyapatite and beta-tricalcium phosphate. Mater Sci Eng C. 2017;75:798–806. DOI: 10.1016/j.msec.2017.02.065
10. Chen J, Ashames A, Buabeid MA, Fahelelbom KM, Ijaz M, Murtaza G. Nanocomposites drug delivery systems for the healing of bone fractures. Int J Pharm. 2020;585:119477. DOI: 10.1016/j.ijpharm.2020.119477
11. Bohner M, Santoni BL, Döbelin N. β-tricalcium phosphate for bone substitution: Synthesis and properties. Acta Biomater. 2020;113:23-4. DOI: 10.1016/j.actbio.2020.06.022
12. Costa SO, Silva PF, Carvalho GG, Almeida YA, Farias JS, Braga AN. A brief review of beta-tricalcium phosphate (β-TCP) doped with metal ions. Am J Eng Res. 2021;10(8):333–44. [available at]
13. Kang HJ, Makkar P, Padalhin AR, Lee GH, Im S Bin, Lee BT. Comparative study on biodegradation and biocompatibility of multichannel calcium phosphate-based bone substitutes. Mater Sci Eng C. 2020;110. DOI: 10.1016/j.msec.2020.110694
14. Kamal RA, Salim R. Assessment of bone density around dental implants using two platelet-rich fibrin protocols (a comparative clinical study). Al-Rafidain Dent J. 2022;22(2):280-91. DOI: 10.33899/rden.2021.128683.1058

15. Dashore S, Chouhan K, Nanda S, Sharma A. Platelet-rich fibrin, preparation and use in dermatology. Indian Dermatol Online J. 2021;12(7):S55–65. DOI: 10.4103%2Fidoj.idoj_282_21
16. Chakrapani S, Sirisha K, Srilalitha A, Srinivas M. Choice of diagnostic and therapeutic imaging in periodontics and implantology. J Indian Soc Periodontol. 2023;17(6):711. DOI: 10.4103%2F0972-124X.124474
17. Shah N, Bansal N, Logani A. Recent advances in imaging technologies in dentistry. World J Radiol. 2014;6(10):794–807. DOI: 10.4329/wjr.v6.i10.794
18. Campos MJ. Bone mineral density in cone beam computed tomography: Only a few shades of gray. World J Radiol. 2014;6(8):607. DOI: 10.4329%2Fwjr.v6.i8.607
19. Pauwels R, Jacobs R, Singer SR, Mupparapu M. CBCT-based bone quality assessment: Are Hounsfield units applicable?. Dentomaxillofac Radiol. 2015;44(1):20140238 DOI: 10.1259/dmfr.20140238
20. Huang H, Chen D, Lippuner K, Hunziker EB. Human bone typing using quantitative cone-beam computed tomography. Int Dent J. 2023;73(2):259-66. DOI: 10.1016/j.identj.2022.08.011
21. Basha SM, Shawky HA, Hanafi R. Radiographical and immunohistochemical evaluation of silver nanoparticles in treatment of intra-osseus defects. An animal study. Egypt Dental J. 2015;61(3). [available at]
22. Shao Z, Lyu C, Teng L, Xie X, Sun J, Zou D. An injectable fibrin scaffold rich in growth factors for skin repair. Biomed Res Int. 2021;2021. DOI: 10.1155/2021/8094932
23. Mourão CF, Lowenstein A, Mello-Machado RC, Ghanaati S, Pinto N, Kawase T, Alves GG, Messora MR. Standardization of animal models and techniques for platelet-rich fibrin production: A narrative review and guideline. Bioeng. 2023;10(4):482. DOI: 10.3390/bioengineering10040482
24. Allawi AH. Clinical and ultrasonographic study of using autogenous venous graft and platelet-rich plasma for repairing Achilles tendon rupture in dogs. Iraqi J Vet Sci. 2019;33(2):453–60. DOI: 10.33899/ijvs.2019.163199
25. Razi T, Emamverdizadeh P, Nilavar N, Razi S. Comparison of the Hounsfield unit in CT scan with the gray level in cone-beam CT. J Dent Res Dent Clin Dent Prospects. 2019;13(3):177. DOI: 10.15171/joddd.2019.028
26. Allawi AH, Saeed MG. Effect of homologous platelet rich fibrin matrix and injectable platelet rich fibrin on full thickness skin autograft healing in dogs. Iraqi J Vet Sci. 2023;37(I-IV):55-64. DOI: 10.33899/ijvs.2022.1371380.2643
27. Kour P, Pudakalkatti PS, Vas AM, Das S, Padmanabhan S. Comparative Evaluation of antimicrobial efficacy of platelet-rich plasma, platelet-rich fibrin, and injectable platelet-rich fibrin on the standard strains of *Porphyromonas gingivalis* and *Aggregatibacter actinomycetemcomitans*. Contemp Clin Dent. 2018;9(٢). DOI: 10.4103%2Fccd.ccd_367_18
28. Atiyah AG, Alkattan LM, Shareef AM. The radiological study of using fabricated calcium hydroxide from quail eggshell and plasma-rich fibrin for reconstitution of a mandibular bone gap in dogs. Iraqi J Vet Sci. 2024;38(1):55-62. DOI: 10.33899/ijvs.2023.139898.2998
29. Zedan IA, Alkattan LM, Al-Mahmood SS. Histopathological and immunohistochemical assessment of the using platelets rich fibrin to reinforce ventral hernioplasty in the sheep model. Iraqi J Vet Sci. 2023;37(4):821-9. DOI: 10.33899/ijvs.2023.139183.2900
30. Ghanaati S, Booms P, Orlowska A, Kubesch A, Lorenz J, Rutkowski J, Landes C, Sader R, Kirkpatrick CJ, Choukroun J. Advanced platelet-rich fibrin: A new concept for cell-based tissue engineering by means of inflammatory cells. J Oral Implantol. 2014;40(6):679–89. DOI: 10.1563/aaid-joi-D-14-00138
31. Abdulmawjood YF, Thanoon MG, Ibrahim SM, Alsofy JH. Histopathological study about the effect of nano magnesium oxide and platelets rich fibrin on the healing of induced radial fracture in dogs. Iraqi J Vet Sci. 2022;36:123-30. DOI: 10.33899/ijvs.2022.135761.2516
32. Jasmine S, Thangavelu A, Janarthanan K, Krishnamoorthy R, Alshatwi AA. Antimicrobial and antibiofilm potential of injectable platelet rich fibrin—a second-generation platelet concentrate—against biofilm producing oral staphylococcus isolates. Saudi J Biol Sci. 2020;27:41–46. DOI: 10.1016/j.sjbs.2019.04.012
33. Bee SL, Bustami Y, Ul-Hamid A, Lim K, Abdul Hamid ZA. Synthesis of silver nanoparticle-decorated hydroxyapatite nanocomposite with combined bioactivity and antibacterial properties. J Mater Sci Mater Med. 2021;32. DOI: 10.1007/s10856-021-06590-y
34. Zhang Y, Cao C, Li J, Liu C, Mi K, Zhang X. Platelet-rich fibrin combined with new bone graft material for mandibular defect repair: A in vivo study on rabbits. Dent Mater J. 2023. DOI: 10.4012/dmj.2022-076
35. Slane J, Vivanco J, Rose W, Ploeg HL, Squire M. Mechanical, material, and antimicrobial properties of acrylic bone cement impregnated with silver nanoparticles. Mater Sci Eng. 2015;48:188–96. DOI: 10.1016/j.msec.2014.11.068
36. Bruna T, Maldonado-Bravo F, Jara P, Caro N. Silver nanoparticles and their antibacterial applications. Int J Mol Sci. 2021;٧٢٠٢:(١٣)٢٢;٤. DOI: 10.3390/ijms22137202
37. El-shafey SA, El-Mezyen AE, Behery AS, Abd El Raouf M. Comparing efficacy of the platelet rich plasma and advanced platelet rich fibrin on tibial bone defect regeneration in dogs. Iraqi J Vet Sci. 2022;36(4):973-80. DOI: 10.33899/ijvs.2022.132765.2129
38. Zhang Y, Shu T, Wang S, Liu Z, Cheng Y, Li A. The osteoinductivity of calcium phosphate-based biomaterials: A tight interaction with bone healing. Front Bioeng Biotech. 2022;16:10. DOI: 10.3389/fbioe.2022.911180
39. Abdulmawjood YF, Thanoon MG. A comparative study of nano magnesium oxide versus platelets rich fibrin to repair the induced radial fracture in dogs. Iraqi J Vet Sci. 2022;36(2):451-8. DOI: 10.33899/ijvs.2021.130500.1836
40. Raffea NM, Allawi AH. Effect of autologous peritoneum and platelet-rich fibrin graft on healing of intestinal anastomosis in dogs. Iraqi J Vet Sci. 2022;36(2):459-470. DOI: 10.33899/ijvs.2021.130529.1840

تأثير بديل العظام النانوية مع الليفين الغني بالصفيحات الدموية القابلة للحقن على التئام عيوب عظم الفك السفلي: دراسة تجريبية على الكلاب

علياء إسماعيل ناصر[١]، ريان سالم حامد[١] و غادة عبدالرحمن طاقة[٢]

[١]فرع جراحة الفم والوجه والفكين، [٢]فرع العلوم الأساسية لطب الأسنان، كلية طب الأسنان، جامعة الموصل، الموصل، العراق

الخلاصة

تناولت هذه الدراسة الاستجابة البيولوجية لعظم الفك السفلي في الكلاب تجاه مادة مركبة نانوية اصطناعية بمفردها أو بالاشتراك مع الليفين الغني بالصفيحات الدموية القابلة للحقن. تم استخدام اثني عشر كلبا من السلالات المحلية من الذكور البالغين الأصحاء تتراوح أعمارهم بين ١٢ إلى ١٨ شهرا وأوزانهم من ١٥ إلى ٢٠ كجم في الدراسة. بناء على فترات الشفاء التي تتراوح بين شهر وشهرين، تم تقسيم هذه الكلاب إلى مجموعتين .كان لكل مجموعة ٤ مجموعات فرعية تضم كل منها ٣ كلاب واعتمد التقسيم على المادة المستخدمة واعتبرت المجموعة الأولى مجموعة سيطرة سالبة ومجموعة الليفين الغني بالصفيحات الدموية القابلة للحقن ومجموعة ١٠حقن المركب النانوي، ومجموعة الليفين الغني بالصفيحات الدموية القابلة للحقن مع المركب النانوي. تم قبل الجراحة سحب دم بمقدار ١٠ مل من الوريد الوداجي حيوان لتحضير الليفين الغني بالصفيحات الدموية القابلة للحقن وتم بعد ذلك خلط الليفين

الغني بالصفيحات الدموية القابلة للحقن مع مادة البحث النانوية لتكوين قوام يشبه الهلام. بدأ الجزء الجراحي بعمل شق متوازي بطول ٥ سم على طول الحافة الخلفية السفلية للفك السفلي. بعد كشف العظم تم عمل ثلاثة ثقوب بقطر ٥ ملم وعمق ٥ ملم ومسافة ٥ملم بين ثقب وأخر، تم وضع المادة في الثقوب الثلاثة للحيوان الواحد. تمت تغطية الثقوب لكل المجاميع بأغشية كولاجين قابلة للامتصاص متبوعة بخياطة السديلة المخاطية السمحاقية. أظهر التحليل الإحصائي اختلافات كبيرة للغاية بين المجموعات، حيث حصلت مجموعة الليفين الغني بالصفيحات الدموية القابلة للحقن مع المركب النانوي على أعلى المتوسطات ٣٣٢,٦٦ و٥٢٢,٦٦ في الشهر الأول والثاني. أدى الليفين الغني بالصفيحات الدموية القابلة للحقن والمركب النانوي عن طريق الحقن إلى زيادة كثافة العظام.